Optical Properties of Poly(2,6-Dimethyl-1,4-Phenylene Oxide) Film and its Potential for a Long-Term Solar Ultraviolet Dosimeter

Lester, R.A.[1], Parisi, A.V.[1*], Kimlin, M.G.[1,2] and Sabburg, J.[1]

[1]Centre for Astronomy, Solar Radiation and Climate, University of Southern Queensland, Toowoomba, Australia
[2]National Ultraviolet Monitoring Centre, Department of Physics and Astronomy, University of Georgia, Athens, USA

*Correspondence: Ph: +61(0) 7 4631 2226 Fax: +61(0) 7 4631 2721 Email: parisi@usq.edu.au

Short Title: UV Dosimetry Using PPO film

Lester, R.A. and Parisi, Alfio and Kimlin, M.G. and Sabburg, J. (2003) *Optical Properties of Poly(2,6-Dimethyl-1,4-Phenylene Oxide) Film and its Potential for a Long-Term Solar Ultraviolet Dosimeter*. Physics in Medicine and Biology, 48. pp. 3685-3698.
Author's final manuscript version. Accessed from USQ ePrints http://eprints.usq.edu.au

Abstract

The optical properties of poly(2,6-dimethyl-1,4-phenylene oxide) (PPO) film have been characterised in order to develop an alternative method for UV dosimetry with a focus on long-term human exposure measurements. The dynamic range of PPO film was found to extend to 2 MJm^{-2} of broadband UV exposure independently of film thickness, providing an exposure range of roughly four summer days at subtropical latitudes. The sensitivity of the film to UV exposure was positively related to film thickness in the 20 to 40 μm range. Films of 40 μm thickness proved to be the most suitable for long-term human UV exposure measurements.

The temperature independence of the response of 40 μm PPO film was established from 1.5°C to 50°C within a dosimeter response uncertainty of 6.5%. Dose-rate independence was also demonstrated within 8% of the mean dosimeter response. The spectral response approximates the CIE erythemal action spectrum between 300 and 340 nm, with a peak response at 305 nm. A large deviation from this action spectrum was observed at shorter wavelengths. Investigation of the angular response in both the azimuth and altitude planes showed a cosine error of less than 6.2% between 0° and 40°, and did not exceed 13.3% at any angle greater than 40°. These results indicate that PPO film satisfies the requirements for use as a UV dosimeter, and may be employed in long-term human exposure measurements.

1 Introduction

The skin and eyes of humans are unavoidably exposed to solar ultraviolet (UV) radiation for various periods throughout normal life. Small exposures are important, acting as a catalyst in the formation of dermal vitamin D (Webb 1993). Over-exposure to UV however, is detrimental. The UVB waveband (280 to 315 nm) typically comprises only about 5% of the total solar UV. However, this waveband accounts for most UV-induced biological effects. Acute over-exposure to UVB, for example, induces rapid biological reactions including erythema and photokeratitis. Chronic exposures to this waveband have been linked to diseases such as photoaging, basal cell and squamous cell carcinomas, and cataracts (Longstreth *et al* 1998).

Natural protection from harmful solar UVB radiation provided by the atmosphere has declined over the past two decades with decreasing stratospheric ozone levels, due to anthropogenic emissions of ozone depleting substances (McKenzie *et al* 1999). An inverse exponential relationship exists between biologically damaging UV radiation and stratospheric ozone concentration (Madronich *et al* 1998), and also between the incidence of skin cancer and UVB irradiance (van der Leun & de Gruijl 2002). The downward trend in stratospheric ozone over this period has therefore raised concerns about the levels of biologically damaging radiation encountered at the earth's surface and its effect on human health. In response, the demand for cost and labour effective UV quantification methods has increased.

Two primary methods of UV quantification have traditionally been employed. These are the employment of various photosensitive films in passive UV dosimetry, and UV radiometry, in which electronic detectors are employed. The costs, labour and logistics of passive UV dosimetry are favourable over radiometric methods for exposure quantification over complex shapes such as the human form (Parisi & Wong 1999; Terenetskaya 1999). Polysulphone film has been applied extensively for such applications (Diffey *et al* 1982; Diffey 1989; Lester & Parisi 2002; Kimlin & Parisi 1999) due to its low cost, availability and ease of use, and the

resemblance of the spectral response to the erythemal action spectrum (CIE 1998; Davis *et al* 1976). After a certain UV exposure is reached, UV polysulphone dosimeters fail to respond to further exposure due to optical saturation. This is a disadvantage of polysulphone film in long-term UV exposure measurements, as it saturates within one summer day at mid-latitudes (CIE 1998; Diffey 1989).

PPO film dosimeters have previously been employed for long-term UV exposure measurements (Bere & Lala 1989). The dose-response and temperature independence of PPO film was investigated in this work. The research presented in this paper additionally examines the angular response, spectral response, dose-rate effects and the dark reaction of PPO film in order to maximise the effectiveness of PPO film as a UV dosimeter. The tensile and optical properties of different film thicknesses are also investigated. The optical properties for a given film thickness are then fully characterised, such that PPO film can be applied in the long-term dosimetry of human solar UV exposure.

2 Materials and Methods

2.1 PPO Dosimeter Fabrication

PPO dosimeter films were fabricated by dissolving PPO powder in chloroform ($CHCl_3$) and applying the solution to a polymer casting-table. The casting-table is comprised of a highly polished glass plate and a steel casting-blade that is driven across the glass. The casting-blade spreads the solution into a thin uniform layer over the glass, from which the $CHCl_3$ evaporates, leaving a thin film of PPO. Films were cast at thicknesses of 15, 20, 40, 50 and 60 μm by adjusting the distance between the glass and the casting-blade.

A PPO mass to $CHCl_3$ volume ratio (mixing ratio) of 0.12 was used for each film thickness except the 15 μm thick film, for which the mixing ratio was 0.14. An additional film of 20 μm thickness was cast using a mixing ratio of 0.06 in order to investigate the effect of the mixing ratio on the film's dose response. The films were cut to size to cover a 12 × 16 mm aperture of a 30 × 30 mm PVC holder, forming PPO film dosimeters.

The durability of PPO film in terms of tear-resistance and brittleness was quantified subjectively by observing the ease at which tearing and fractures occurred during removal of the film from the casting table. Visual inspection was used to assess the quality of the film in terms of surface blemishes.

2.2 Irradiation Sources

The UV radiation sources used in the optical characterisation of PPO film dosimeters included natural solar UV radiation, simulated solar UV radiation (model 15S solar UV simulator, Solar Light Co., Philadelphia, USA), fluorescent UV (FUV) lamp radiation (model FS40/12, Philips, Lawrence & Hanson, Toowoomba, Australia), and monochromatic radiation from an irradiation monochromator. The irradiation monochromator is comprised of an LX/450-2 xenon arc lamp and a GM 252 single monochromator supplied by Spectral Energy, New Jersey, USA. The output of the solar UV simulator and the irradiation monochromator are collimated. Due to the small spot diameters of these instruments, dosimeters were exposed to these sources sequentially. Exposure of the entire dosimeter surface at maximum intensity was achieved by adjusting the distance between the output aperture of the collimated sources and the dosimeter to be exposed such that the beam just covered the dosimeter aperture. Larger numbers of dosimeters were simultaneously exposed to the other sources for statistical purposes.

2.3 Irradiance Measurements

Before dosimeters were irradiated, it was necessary to determine the irradiance of the source. An outdoor erythemal meter (model 501 UV-Biometer, Solar Light Co., Philadelphia, USA) was used to monitor solar UV. The 501 UV-Biometer has a response approximating the CIE erythemal action spectrum. This instrument is regularly calibrated in units of minimum erythemal dose (MED) (1 MED = 214 Jm^{-2} for this calibration) against the scanning spectroradiometer (described below) for CIE weighted erythemal irradiance, and has an estimated uncertainty of 10% at best.

In this work, the primary instrument used for measurement of artificial radiation sources was a scanning spectroradiometer. This instrument is comprised of a 15 cm diameter integrating sphere (model OL IS 640, Optronics Laboratories, Orlando, USA), a 1200 lines/mm double holographic grating monochromator (model DH10, Jobin Yvon Co., France) and a UV photomultiplier tube (model R212, Hamamatsu Co., Japan) temperature stabilised to 15.0 ± 0.5°C. The spectroradiometer was calibrated for wavelength against the 365.0 nm mercury emission line of a mercury discharge lamp to within ± 0.1 nm, and against an air-cooled secondary standard quartz-tungsten halogen lamp for spectral irradiance. The secondary standard was powered by a Kenwood regulated power supply (model PD36 20AD) at a current of 9.500 ± 0.005 A, monitored by a calibrated MX 56 Metrix multimeter. The secondary standard irradiance is traceable to the National Standards Laboratory at the CSIRO, Lindfield, Australia. The estimated uncertainty in absolute spectral irradiance measurements is 10%.

The spectral response of the spectroradiometer was determined by performing a dark scan, and a secondary standard scan over the desired waveband using the appropriate wavelength increment, $d\lambda$. The integrating sphere and monochromator were maintained in complete darkness during the dark scans.

The irradiance I was calculated as

$$I = \int_{\lambda_1}^{\lambda_2} I(\lambda) d\lambda \tag{1}$$

where λ_1 and λ_2 are short and long wavelength limits respectively of the waveband of interest and $I(\lambda)$ is the measured spectral irradiance. The values of λ_1 and λ_2 were set to 280 and 400 nm respectively and a $d\lambda$ of 1 nm was used in the measurement of all radiation sources except the irradiation monochromator. In this case, the irradiation monochromator output wavelength of interest was selected, and λ_1 and λ_2 were set 10 nm below and 10 nm above this wavelength respectively. Due to the small full width half maximum (FWHM) of the irradiation monochromator, accurate irradiance calculations required a $d\lambda$ of 0.1 nm.

2.4 Optical Density Measurements

The optical density spectra ($OD(\lambda)$) was measured by scanning the optical density (OD) from 300 to 400 nm at 1 nm increments using a UV-1601 Shimadzu spectrophotometer. The manufacturer specified uncertainty of this instrument for OD measurements is ± 0.002. The $OD(\lambda)$ were determined before and after exposure of the dosimeters to UV radiation to give the change in optical density spectrum

$$\Delta OD(\lambda) = OD_a(\lambda) - OD_b(\lambda) \tag{2}$$

where $OD_b(\lambda)$ is the optical density spectrum before exposure and $OD_a(\lambda)$ is that after exposure. Possible effects of dust or small film defects on the $OD(\lambda)$ measurements were minimised by measuring the $OD(\lambda)$ at four different orthogonal orientations of the spectrophotometer beam with respect to the film surface and averaging these measurements. The spectrophotometer beam orientations were identical for measurements of both $OD_b(\lambda)$ and $OD_a(\lambda)$, eliminating the effects of unquantified variations in irradiance across the beam of the collimated sources. After the most suitable spectrophotometer wavelength (λ_{SP}) was determined for $\Delta OD(\lambda)$ measurements, λ_{SP} was substituted for λ in equation (2), and fixed wavelength measurements of $\Delta OD(\lambda_{SP})$ were determined.

2.5 PPO Dose-Response and Calibration Curves

Dose-response curves were obtained for the radiation sources described above. The solar UV simulator and irradiation monochromator curves were produced by exposing a single dosimeter to the given UV source for a long period, during which, the $\Delta OD(\lambda_{SP})$ was determined at regular time intervals. The exposure periods for the solar UV simulator and irradiation monochromator were 5 hours and 30.6 hours respectively, with $\Delta OD(\lambda_{SP})$ measurements respectively at half-hourly and hourly intervals. The $\Delta OD(\lambda_{SP})$ at each time interval was plotted against the cumulative exposure H, received by the dosimeter at the end of that interval. The cumulative exposure was calculated as

$$H = It \tag{3}$$

where I is the irradiance (calculated by equation (1)) and t is exposure time until the end of the last exposure interval. Dose-response curves for the FUV lamp and natural solar radiation were determined by exposing 24 to 25 dosimeters to the given source. One dosimeter at a time was removed from the exposure at regular time intervals ranging from 0.5 hours to 8 hours. The time intervals were slowly increased with increasing exposure. The $\Delta OD(\lambda_{SP})$ was determined for each dosimeter and plotted against cumulative exposure. In the case of natural solar radiation, the axes of the dose-response curve were inverted to provide the cumulative erythemal exposure as a function of $\Delta OD(\lambda_{SP})$. This calibration was determined over a period of 17 days during August 2002, at the University of Southern Queensland, Toowoomba, Australia (27.6 S).

2.6 Reproducibility

The ability of a dosimeter to resolve UV exposures depends on the UV exposure reproducibility provided by the dosimeter. The reproducibility was evaluated by determining a dose-response curve using the method employed for determining dose-response curves for the solar UV simulator and the irradiation monochromator, described in section 2.5. In this experiment however, 14 dosimeters were simultaneously exposed to the FUV lamp for a period of 84 hours. The $\Delta OD(\lambda_{SP})$ was determined at half-hourly intervals during the first 5 hours, and then at 12-hourly intervals for the remaining exposure time. The mean and standard deviation of the $\Delta OD(\lambda_{SP})$ were calculated, to provide the coefficient of variation (CV) as a function of UV exposure.

2.7 Temperature Effects and Dark Reaction

Environmental conditions govern the temperature at which dosimeters are exposed to solar radiation. In order to determine the effect of temperature on the UV-induced response of PPO film dosimeters, six batches of ten PPO film dosimeters were suspended from a floating platform in a heated water bath at a depth of 1.5 cm. Each batch was exposed to the same UV exposure from the FUV lamp at a different water temperature. These temperatures were 1.5°C,

10°C, 20°C, 30°C, 40°C and 50°C. Temperatures below 30°C were maintained by an immersion cooler. After exposure, the mean $\Delta OD(\lambda_{SP})$ of each batch was determined and compared.

For accurate UV exposure measurements, it is also necessary to understand the post-exposure behaviour of the dosimeter film, and the effect of temperature on such behaviour. Davis *et al* (1976), and Kollias and Baqer (1986) observed a continued increase in the OD of polysulphone after termination of UV exposure, commonly known as the dark reaction. It has been implicitly assumed that the dark reaction is independent of exposure (Davis *et al* 1976; Diffey 1989). This assumption was tested by exposing four pairs of dosimeters each to 162, 544, 950 and 1495 kJm^{-2} of broadband UV from the FUV lamp. The dosimeters were maintained at a temperature of 24°C during and after exposure. Measurements of $OD(\lambda_{SP})$ of each pair of dosimeters were conducted at various intervals for 18 to 22 days after the exposure. The percent increase in $OD(\lambda_{SP})$ resulting from the dark reaction after the four different exposures were determined and compared at each time interval. In addition, the effect of temperature on the dark reaction was investigated by simultaneously exposing four pairs of dosimeters to the FUV lamp administering an exposure of 729.5 kJm^{-2}. The mean $OD(\lambda_{SP})$ of each pair was determined immediately after exposure. Each pair was then maintained at different temperatures of 40°C, 20-24°C, 2°C and -16°C. The mean $OD(\lambda_{SP})$ of each pair was remeasured at various times up to one month after the initial exposure. The percent increase in $OD(\lambda_{SP})$ was then determined as a function of post-exposure time.

2.8 Angular Response

Solar radiation is comprised of both direct and diffuse irradiance. Direct irradiance emanates from the direction of the sun, while diffuse irradiance is scattered in all directions by atmospheric constituents. The response of the dosimeter to UV radiation intercepting the film at different angles (angular response) must therefore be quantified.

The response of an ideal detector to a collimated uniform irradiance source decreases in proportion to the cosine of the angle of incidence of the beam. The cosine error is the deviation of the angular response of the detector from the cosine function. The cosine error of PPO film dosimeters was determined by irradiating dosimeters at angles ranging from 0° to 80° in the azimuth plane, and from 0° to 70° in the altitude plane at intervals of 10° with the collimated beam of the solar UV simulator. Normal incidence (0°) was defined by placing a small plane mirror in the dosimeter holder, and aligning the reflected beam with the centre of the output aperture of the solar UV simulator. The $\Delta OD(\lambda_{SP})$ was determined for each dosimeter and the normalised response R_N was calculated as

$$R_N = \frac{-8.2x^3 + 18.0x^2 + 1.7x}{-8.2x_0^{\,3} + 18.0x_0^{\,2} + 1.7x_0} \qquad (4)$$

where x is the $\Delta OD(\lambda_{SP})$ induced at any angle and x_0 is the $\Delta OD(\lambda_{SP})$ induced at normal incidence. The numerator and denominator of (4) are the dose-response equation for the solar UV simulator. Such a normalisation is required in order to account for nonlinearity in the dose-response.

2.9 Reciprocity

The response of a UV dosimeter must reasonably satisfy the reciprocity law within the range of exposures for which its use is intended. This law states that a UV-induced response due to a given UV exposure is the same, regardless of the exposure time and irradiance. The response

of a UV dosimeter must therefore be proportional to the product of UV exposure time and irradiance.

The spectroradiometer was used to measure the output of the FUV lamp at six different distances from the fluorescent tube in random order. The decrease in irradiance with increase in height was used to investigate the effects of different irradiance and exposure times on the $\Delta OD(\lambda_{SP})$ for a given exposure. One batch of dosimeters (10 per batch) was exposed at a distance of 6 cm from the fluorescent tube for 55.4 hours, giving these dosimeters an exposure of 1.9 MJm^{-2}. Equation (3) was employed to calculate the time required for batches irradiated at distances of 17, 32, 42 and 52 cm from the tube to receive the same dose. The required exposure times ranged from 55 hours to 487 hours. The mean $\Delta OD(\lambda_{SP})$ was determined and compared after the exposure of each batch.

2.10 Spectral Response

Input and output slit widths of 1 mm on the irradiation monochromator provided an output of 2.2 Wm^{-2} at 280 nm with a general increase to 3.2 Wm^{-2} at 340 nm as measured with the spectroradiometer. The FWHM was 4.1 nm and independent of wavelength. In order to determine the spectral sensitivity of PPO film, PPO dosimeters were exposed sequentially to this source, receiving a given dose at wavelengths from 280 to 340 nm at 5 nm intervals. The $\Delta OD(\lambda_{SP})$ induced by the UV dose at a given wavelength was substituted into the monochromatic dose-response equation determined at 305 nm and normalised to the measured dose at that wavelength (Diffey 1989; Diffey *et al* 1982). The spectral response exposures were repeated two or three times at most wavelengths. The reproducibility of the dosimeter response at any given wavelength was within 8.8%.

3 Results

3.1 PPO Dosimeter Fabrication – Thickness, Durability and Film Quality

The durability and tear-resistance of PPO dosimeters increased with film thickness up to 40 μm, whereas 50 and 60 μm films were brittle. The brittleness of these films could be reduced by increasing the mixing ratio. However, the required mixing ratio of greater than 0.16 was difficult to cast due to the long time requirement for the PPO powder to dissolve, and the high viscosity of the solution. Films of 15 μm thickness were very fragile and could not be cast using a mixing ratio of less than 0.14.

Visual inspection of the films indicated that the film quality, in terms of an absence of surface blemishes and defects, was greatest for films of 20 and 40 μm thickness when cast using a mixing ratio of 0.16. Due to ease of casting, high quality, and high UV sensitivity (next section), a film thickness of 40 μm was selected for further research.

3.2 PPO Film Thickness and Dose-Response Curves

Dose response curves for five different film thicknesses are presented in Figure 1. $\Delta OD(\lambda_{SP} =$ 340 nm) was used for this experiment according to Berre and Lala (1989); Lala (1984). However, the λ_{SP} is revised in the next section. The dose-response curves of two 20 μm films (Figures 1(b) and 1(c)) fabricated using mixing ratios of 0.06 and 0.12 are virtually indistinguishable, indicating that the mixing ratio has no effect on the dose-response of the film. A marked increase of the sensitivity of the film to UV exposure is seen with increasing film thickness. It is clear from Figure 1 that the dose-response of 15 and 20 μm films is near linear for exposures up to about 1200 kJm^{-2}, whereas, the response of the thicker films is strongly nonlinear in this region, particularly between 0 and 300 kJm^{-2}.

Resulting from optical saturation, the rate of increase of the ΔOD decreases after large exposures (Diffey 1989). This rate of change is similar for all curves in Figure 1 at exposures greater than about 1200 kJm^{-2}, indicating that the point of saturation is independent of film thickness.

3.3 Change in Optical Density Spectra and Measurement Wavelength

The $\Delta OD(\lambda)$ of dosimeters of 40 μm film thickness due to UV exposure shows a maximum at 302 nm which shifts to longer wavelengths with increasing exposure (307 nm after an exposure of 2310 kJm^{-2}) (Figure 2). The greatest $\Delta OD(\lambda)$ at longer wavelengths occurs at approximately 320 nm. This region of the curve does not shift significantly with increasing exposure, as does the 302-307 nm maxima, and is thus used for λ_{SP} in all subsequent experiments.

3.4 Solar UV Calibration

Figure 3 shows the cumulative erythemal UV exposure ranging from 0 to 148 MED plotted against $\Delta OD(320)$ of 40 μm thick PPO film dosimeters. The solid line represents the cubic function

$$UV_{Er} = 0.337x^3 + 1.11x^2 + 37.9x \text{ (MED)} \quad (5)$$

where UV_{Er} is the solar UV exposure weighted against the CIE erythemal action spectrum measured using the 501 UV-Biometer, and x is the $\Delta OD(320)$. The R^2 value for this function is 0.994. The film saturates suddenly after an exposure of about 145 MED as indicated by the data points represented by crosses in Figure 3. These data points do not contribute to the UV_{Er} function.

3.5 Reproducibility

The variation of the UV-induced $\Delta OD(320)$ of 40 μm thick PPO film dosimeters gave a CV of less than 4% for broadband exposures up to about 700 kJm^{-2} ($\Delta OD(320) \cong 1.1$). A steady increase in the CV occurred with increasing exposure to a maximum of 6.5% for an exposure of 2582 kJm^{-2} ($\Delta OD(320) \cong 1.9$).

3.6 Temperature Effects and Dark Reaction

The effect of temperature on the UV-induced $\Delta OD(320)$ is shown in Figure 4. Analysis of variance showed no significant differences in dosimeter response at the six different temperature levels ($p < 0.01$). The interdosimeter variation was about 5% at each temperature level, and the variation between temperature levels was less than 2%.

The percent increase in $OD(320)$ due to the dark reaction is plotted against the $\Delta OD(320)$ induced by four different broadband UV exposures at different time intervals after the exposure in Figure 5. A slight inverse dependence of the dark reaction on exposure is evident. A maximum dark reaction induced increase in $OD(320)$ of 3.4% was observed over the exposure range from 162 to 1495 kJm^{-2}. The slopes of the linear regression lines of Figure 5 are similar, indicating that elapsed time after exposure has little effect on the dark reaction-exposure dependence.

The rate of increase of the dark reaction depended on the temperature at which the dosimeters were maintained after exposure (Figure 6). The increase in OD was less than 0.7% at –16°C. The dark reaction at –16°C cannot be distinguished from that at 2°C until about 70 hours after the exposure. The reaction was much higher at warmer temperatures reaching 11% at 24°C and 19% at 40°C after 755 hours.

3.7 Angular Response

The angular response of 40 μm PPO film dosimeters is shown in Figure 7. The Δ*OD*(320) of the dosimeters used in this experiment ranged from 0.17 to 0.55 indicating a CV of less than 4%. Angular alignment errors were estimated to be less than 0.3°. The cosine error ranged from 1.8% to 6.2% for angles smaller than 40°. A maximum error of 13.2% occurred for larger angles up to 80°. Interdosimeter variation may account for nearly 4% of this error.

3.8 Reciprocity

A decreasing trend in the response of PPO film was observed with increasing irradiance from 1.0 to 3.7 Wm^{-2} (Figure 8). The Δ*OD*(320) decreased by about 13% over this range. The response however, remained within the predicted 4% variability from 2.1 to 11.7 Wm^{-2}.

3.9 Spectral Response

The spectral response (Figure 9) shows a maximum wavelength sensitivity of 40 μm thick PPO film at 305 nm. No UV-induced response was observed at wavelengths longer than 340 nm. Exposures in the UVC (270 nm) (not shown) indicate that the response continues to decrease with decreasing wavelength in this region.

4 Discussion

Dose-response curves of PPO films indicate that dosimeters of this type are useful for the quantification of broadband UV exposures of up to about 2 MJm^{-2} before saturation occurs. The OD of thick films (40 to 60 μm) changes more rapidly with broadband UV exposure compared to thin films in the 0 to 1200 kJm^{-2} range. Of the thick films, 40 μm films were logistically easier to cast, and resulted in the development of a dosimeter with a broadband UV detection threshold of less than 17 kJm^{-2}, a large dynamic range of up to 2 MJm^{-2}, and a reproducibility of better than 6.5% over that range.

The essential properties of a solar UV dosimeter are listed by Wong and Parisi (1998). These properties are largely satisfied by PPO film, and hence can be applied as a solar UV dosimeter under most environmental conditions. A film thickness of 40 μm is robust, and the dosimetrically determined UV exposure is independent of temperature. The angular response agrees well with the cosine function in both the azimuth and altitude planes, and the law of reciprocity is satisfied over a large irradiance range. PPO film dosimeters can therefore be employed for UV exposure quantification over a large range of solar zenith angles (SZA) and exposure levels.

When 40 μm thick PPO film dosimeters are deployed on a horizontal plane, the larger cosine errors observed at angles of incidence greater than 40°, and the deviation from reciprocity at low solar irradiance should be considered in relation to both the spectral response of PPO film and the relative intensity of solar radiation at different SZA. At large SZA, the relative proportion of diffuse UVB increases, thereby contributing to the cosine error and detracting from the reciprocity error. The predominant effect of large SZA however, is considerably decreased absolute UVB irradiance compared to that occurring at small SZA. Therefore, under clear-sky conditions, the greatest response of PPO film occurs during small SZA periods. As a result, the low absolute irradiance at large SZA is expected to mitigate both the cosine and reciprocity errors.

In human UV exposure dosimetry however, dosimeters may be oriented at any angle and may be subjected to large differences in irradiance due to the presence or absence of shading at different anatomical sites over the human form. Cosine errors may be as large as 13% for

dosimeters oriented at angles greater than 40° to the direction of the sun. In addition, the low irradiance encountered at constantly shaded sites such as the area under the chin may lead to enhanced reciprocity errors exceeding 13% if the irradiance is less than about 2 Wm^{-2}. In such situations, greater accuracy may be obtained by application of a cosine correction factor, and by using a diffuse irradiance calibration for shaded areas.

An additional property required for UV dosimetry is a spectral response similar to the action spectrum of the biological response of interest (Wong and Parisi 1998). The erythemal action spectrum is perhaps most often considered in human exposure research. The spectral response of PPO film has only a loose resemblance of the CIE erythemal action spectrum. It does however, approximate this action spectrum, and that obtained by Anders *et al* (1995), more closely than polysulphone between 300 and 340 nm. Since solar irradiance is low at wavelengths shorter than 300 nm, errors due to differences between film response and the erythemal action spectrum should not be significant. This disparity may also be reduced by calibrating dosimeters against the cumulative erythemal UV exposure recorded by an appropriate instrument (Diffey 1989).

Dosimeters used for long-term exposure measurements (more than one day) will endure a dark reaction during the nocturnal periods. The nature of the dark reaction over alternating periods of exposure and darkness is currently unclear. A dark reaction however, is expected after each period of exposure, resulting in a cumulative error of up to 3.4% per night for dosimeters receiving different daytime exposures. Correction factors for the dark reaction may be obtained by recording the temperature during each nocturnal period and applying regression equations to data similar to that depicted in Figure 5 determined for the same temperatures as those encountered during the night. After completion of an exposure measurement, the dark reaction may be minimised by performing postexposure $\Delta OD(320)$ measurements immediately after the experiment or by storing exposed dosimeters at a low temperature.

PPO film dosimeters may be employed for long-term human exposure measurements due to their large dynamic range and suitable optical properties. The combined errors associated with calibration, angular response, reciprocity and dark reaction of these dosimeters are estimated to be of the order of 15%. Although less accurate than radiometric methods, PPO film dosimetry provides the versatility required for UV exposure quantification over the human form, and a greater dynamic range than is currently available from chemical film dosimeters.

Acknowledgements
The authors wish to acknowledge Mr Ken Mottram, Mr Graham Holmes, Mr Oliver Kinder and Mr Pat McConnell for their technical assistance, and Prof. John Mainstone for his contribution to the groundwork for this project.

REFERENCES

Anders, A., Altheide, H.-J., Knalmann, M. & Tronnier, H. 1995, 'Action spectrum for erythema in humans investigated with dye lasers,' *Photochemistry and Photobiology*, Vol. 61(2), pp. 200-205.

Berre, B. & Lala, D. 1989, 'Investigation on photochemical dosimeters for ultraviolet radiation,' *Solar Energy*, Vol. 42(5), pp. 405-16.

CIE (International Commission on Illumination) 1998, 'Personal dosimetry of UV radiation,' CIE Technical Report, Publication No. CIE 98.

Davis, A., Deane, G.H.W. & Diffey, B.L. 1976, 'Possible dosimeter for ultraviolet radiation,' *Nature*, Vol. 261, pp. 169-70.

Diffey, B.L. 1982, 'A personal dosimeter for quantifying the biologically effective sunlight exposure of patients receiving benoxaprofen, *Physics in Medicine and Biology*, Vol. 27(12), pp. 1507-13.

Diffey, B.L. 1989, 'Ultraviolet radiation dosimetry with polysulphone film,' in *Radiation Measurement in Photobiology*, ed. B.L. Diffey, pp. 136-59, Academic Press Ltd., New York.

Kimlin, M.G. & Parisi, A.V. 1999, 'Ultraviolet protective capabilities of hats under two different atmospheric conditions,' *2nd Internet Photochemistry and Photobiology Conference, July 16 - Sept 7, 1999.*

Kollias, N. & Baqer, A.H. 1986, 'Measurements of Solar Middle Ultraviolet Radiation in Kuwait,' Environmental Protection Council, Kuwait.

Lala, B. 1984, *Photochemical Measurement of Ultraviolet Radiation*, Proceedings of Recent Advances Pyranometry IEA, Solar R&D, SMHI, Norrkoping, Sweden.

Lester, R.A. & Parisi, A.V. 2002, 'Spectral ultraviolet albedo of roofing surfaces and human facial exposure,' *International Journal of Environmental Health Research*, Vol. 12, pp. 75-81.

Longstreth, J., de Gruijl, F.R., Kripke, M.L., Abseck, S., Arnold, F., Slaper, H.I., Velders, G., Takizawa, Y. & van der Leun, J.C. 1998, 'Health risks,' *Journal of Photochemistry and Photobiology B: Biology*, Vol. 46, pp. 20-39.

Madronich, S., McKenzie, R.L., Bjorn, L.O. & Caldwell, M.M. 1998, 'Changes in biologically active ultraviolet radiation reaching the earth's surface,' *Journal of Photochemistry and Photobiology B: Biology*, Vol. 46, pp. 5-19.

McKenzie, R., Conner, B. & Bodeker, G. 1999, 'Increased summertime UV radiation in New Zealand in response to ozone loss,' *Science*, Vol. 285, pp. 1709-11.

Parisi, A.V, & Wong, J.C.F. 1999, 'Usage of a dosimeter spectrum evaluator for different environments,' Protection Against the Hazards of UVR, Available: http://www.photobiology.com/UVR98/parisi2/index.html [Accessed: July 2, 2002].

Terenetskaya, I.P. 1999, The new method of UV dosimetry based on an in vitro model of previtamin D photosynthesis, *Internet Photochemistry and Photobiology*, Available: http://www.photobiology.com/UVR98/irina/index.htm [Accessed: Feb. 07, 2002].

van der Leun, J.C. & de Gruijl, F.R. 2002, 'Climate change and skin cancer,' *Photochemical Photobiological Sciences*, Vol. 1, pp. 324-6.

Webb, A.R. 1993, 'Vitamin D synthesis under changing UV spectra,' in *Environmental UV Photobiology,* ed. A.R. Young, L.O. Bjorn, J. Moan and W. Nultsch, Plenum Press, New York, pp.185-202.

Wong, J.C.F. & Parisi, A.V. 1998, 'Assessment of ultraviolet radiation exposures in photobiological experiments: Protection against the hazards of UVR,' *Internet Photochemistry and Photobiology* [Online]. [Accessed Sep. 2002].

FIGURE CAPTIONS

Figure 1: Dose-response curves of PPO film dosimeters determined using the OD measurement wavelength of 340 nm for film thicknesses (A) 15 μm, (B) 20 μm fabricated using a mixing ratio of 0.12, (C) 20 μm fabricated using a mixing ratio of 0.06, (D) 40 μm, (E) 50 μm and (F) 60 μm. A total broadband UV (280 to 400 nm) exposure of 2800 kJm^{-2} was administered from the FUV lamp. The dosimeters were exposed to broadband UV (280 to 400 nm) irradiance from the FUV lamp.

Figure 2: $\Delta OD(\lambda)$ of PPO film dosimeters of 40 μm film thickness for exposures of (A) 17 kJm^{-2}, (B) 272 kJm^{-2}, (C) 544 kJm^{-2}, (D) 1223 kJm^{-2} and (E) 2310 kJm^{-2}.

Figure 3: $\Delta OD(320)$ of 40 μm thick PPO film dosimeters calibrated against solar erythemal radiation in units of minimum erythemal dose (MED) defined as 214 Jm^{-2}. The two points marked with crosses are in the region of saturation and do not contribute to the calibration curve.

Figure 4: $\Delta OD(320)$ of PPO film dosimeters of 40 μm film thickness for a given exposure at temperatures ranging from 1.5°C to 50°C. The *x*-error bars represent the temperature variation during the exposure, and the *y*-error bars indicate an interdosimeter variation of about 5%.

Figure 5: The dark reaction induced increase in OD of PPO film dosimeters of 40 μm film thickness as a function of broadband UV exposure. Postexposure *OD*(320) measurements were conducted (A) 17 to 28 hours, (B) 44 to 55 hours, (C) 67 to 77 hours, (D) 92 to 116 hours, (E) 165 to 188 hours and (F) 451 to 536 hours after the exposure. Linear regressions for each time interval are indicated by the solid lines and the *y*-error bars represent the predicted 6% interdosimeter variation.

Figure 6: Dark reaction shown as the percentage increase in the *OD*(320) of PPO film dosimeters of 40 μm film thickness plotted against time since UV exposure. After exposure, the dosimeters were maintained at (A) -16°C, (B) 2°C, (C) 20-24°C and (D) 40°C. The *y*-error bars (too small to be clearly visible at -16°C) represent a predicted interdosimeter variation of 6%.

Figure 7: Azimuth (×) and altitude (○) angular responses of PPO film dosimeters of 40 μm film thickness. The cosine error (●) is presented as the percentage difference between the angular response and the cosine function (right axes). The dashed line represents the cosine function. The *y*-error bars represent the maximum predicted CV of 4%.

Figure 8: $\Delta OD(320)$ of PPO film dosimeters of 40 μm film thickness plotted against the irradiance (●) required to administer an exposure of 1.9 MJm^{-2} over the given exposure period (○) (right axis). The *y*-error bars represent an error of ± 5% that is associated with the irradiance measurements.

Figure 9: Spectral response of PPO film dosimeters of 40 μm film thickness (data points with error bars) compared with the spectral response of polysulphone (solid line), the CIE erythemal action spectrum (dashed line) and the erythemal action spectrum of Anders *et al* (1995) (●). The *x*-error bars indicate the FWHM of the irradiation monochromator output, while the *y*-error bars show the reproducibility of 8.8%.

FIGURES

Figure 1

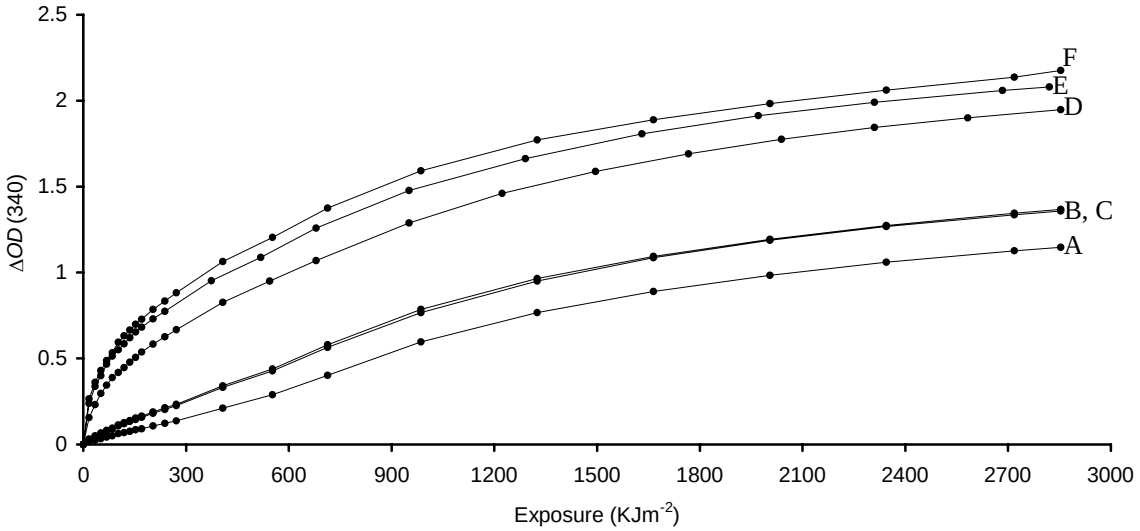

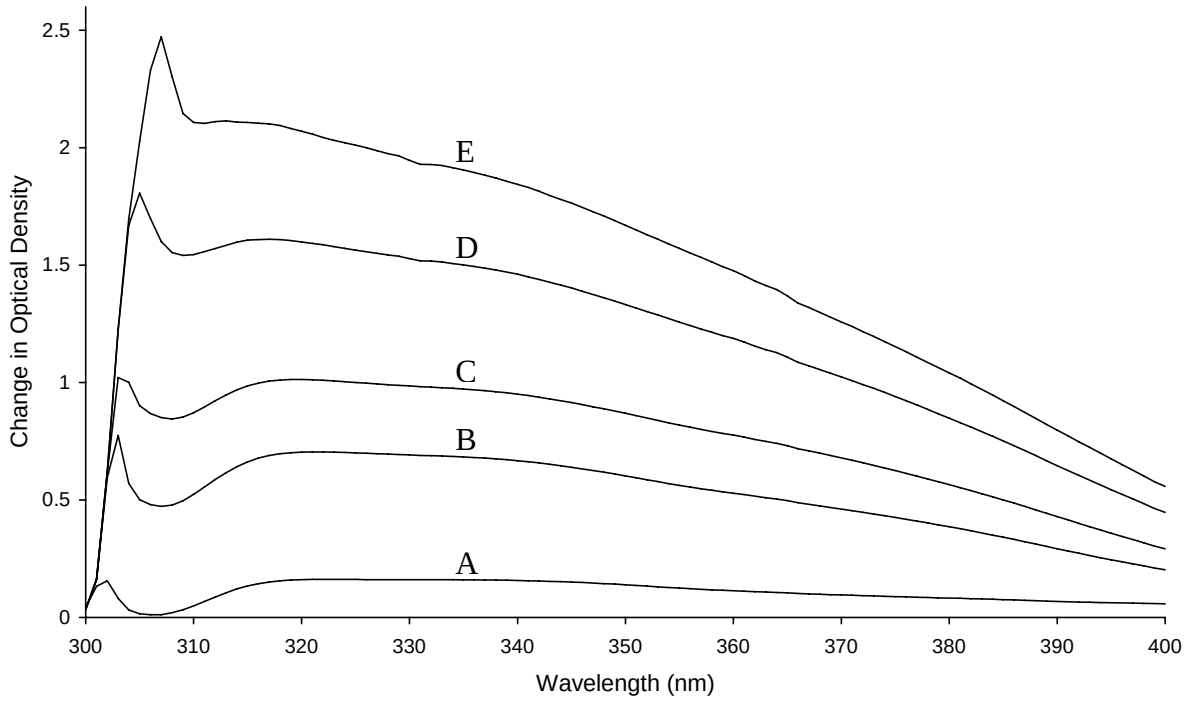
Change in Optical Density
2.5
2
1.5
1
0.5
0
300
310
320
330
340
350
360
370
380
390
400
Wavelength (nm)
E
D
C
B
A

Figure 2

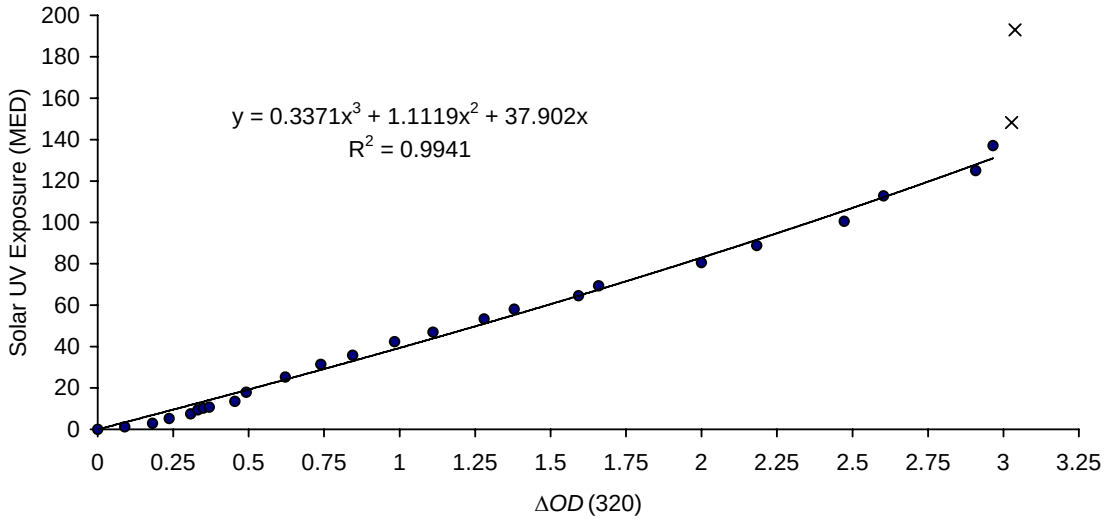
y = 0.3371x3 + 1.1119x2 + 37.902x
R2 = 0.9941
Solar UV Exposure (MED)
ΔOD (320)
0
20
40
60
80
100
120
140
160
180
200
0
0.25
0.5
0.75
1
1.25
1.5
1.75
2
2.25
2.5
2.75
3
3.25

Figure 3

Figure 4

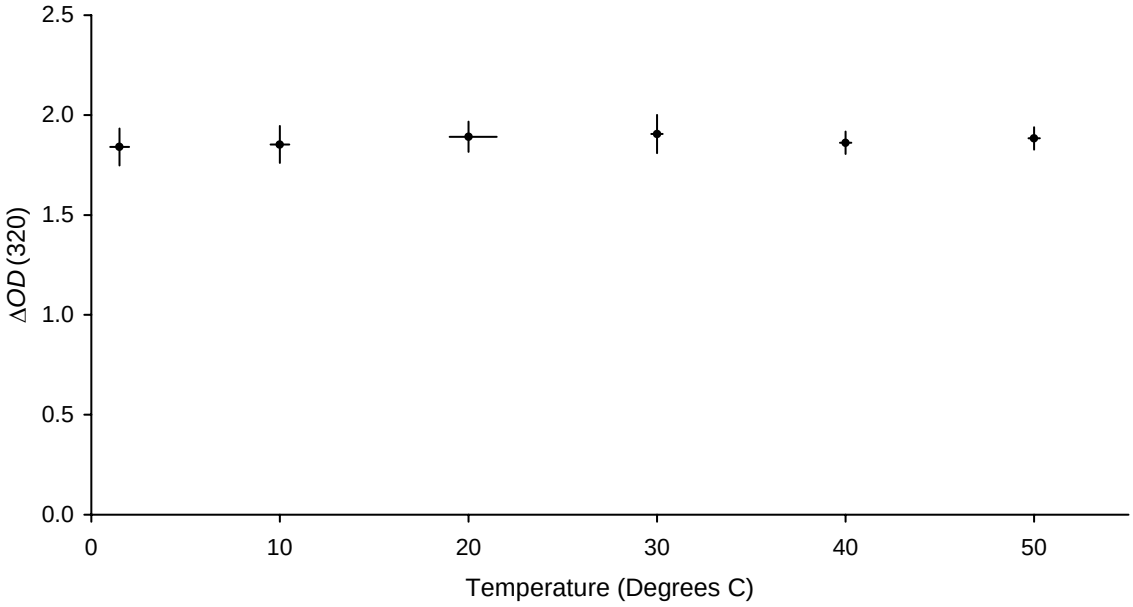

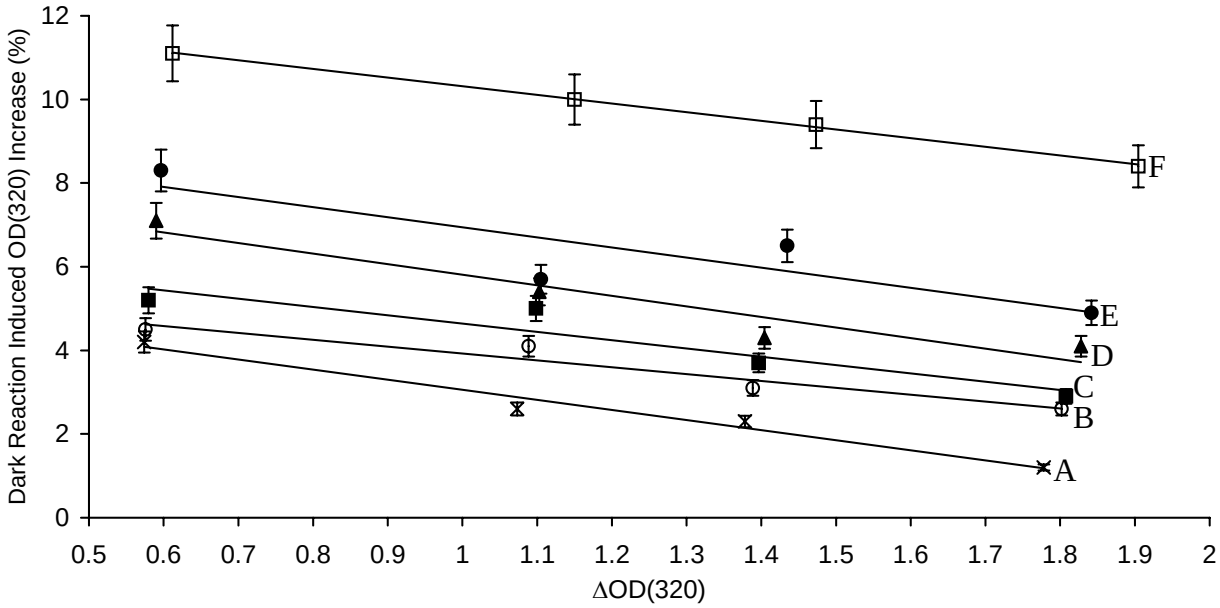
Dark Reaction Induced OD(320) Increase (%)
12
10
8
6
4
2
0
0.5
0.6
0.7
0.8
0.9
1
1.1
1.2
1.3
1.4
1.5
1.6
1.7
1.8
1.9
2
ΔOD(320)
F
E
D
C
B
A

Figure 5

Figure 6

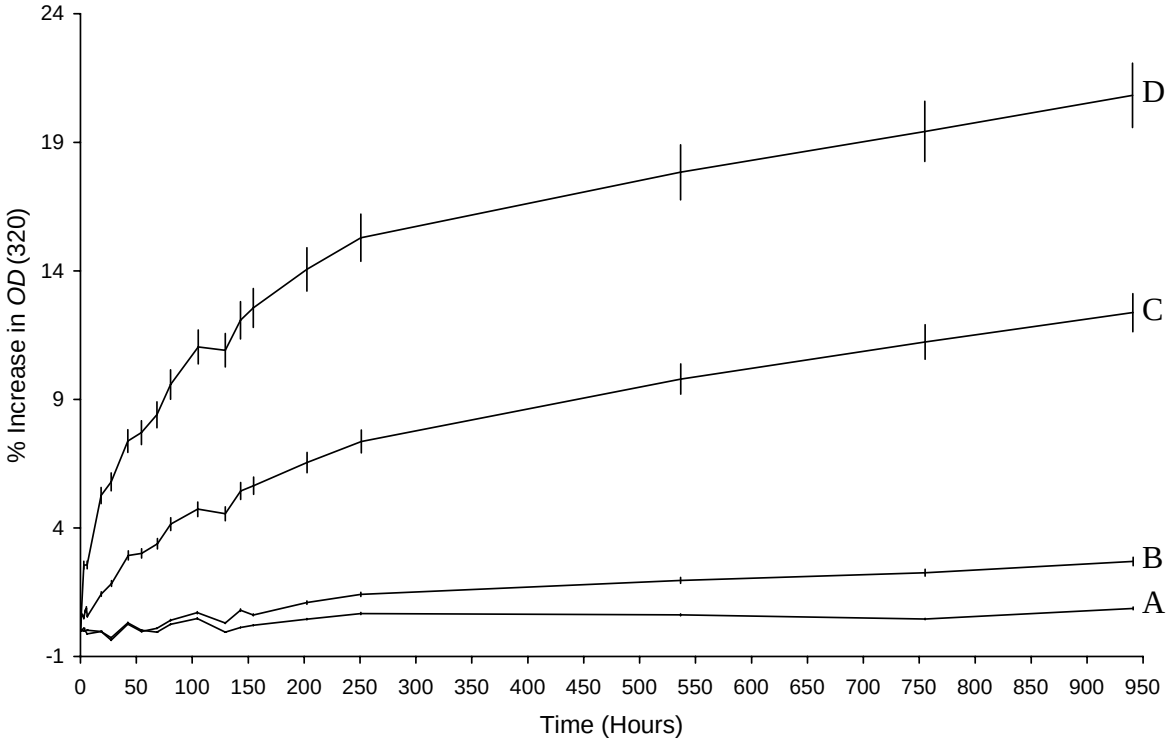
24
19
14
9
4
-1
% Increase in OD (320)
0
50
100
150
200
250
300
350
400
450
500
550
600
650
700
750
800
850
900
950
Time (Hours)
D
C
B
A

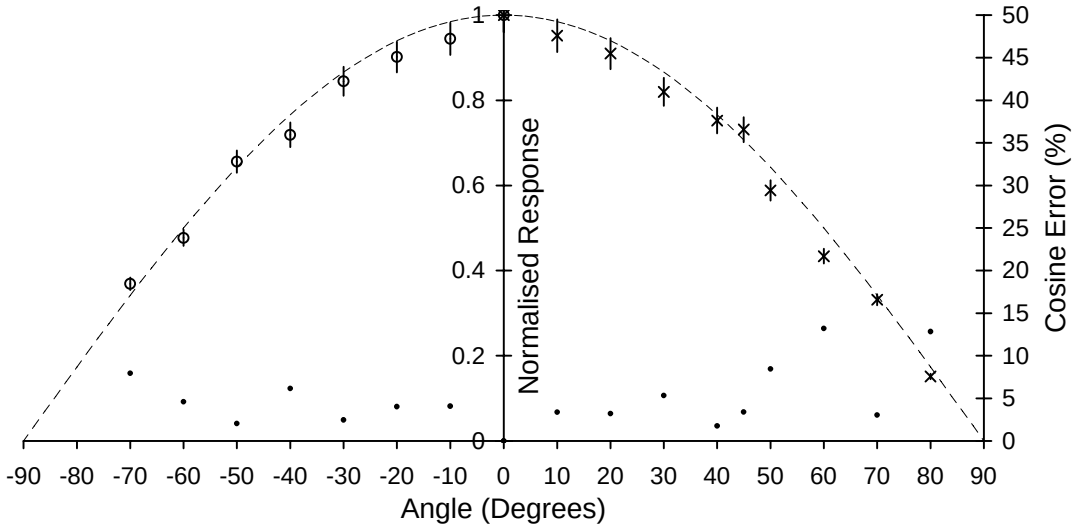
Normalised Response
Cosine Error (%)
Angle (Degrees)
1
0.8
0.6
0.4
0.2
0
50
45
40
35
30
25
20
15
10
5
0
-90 -80 -70 -60 -50 -40 -30 -20 -10 0 10 20 30 40 50 60 70 80 90

Figure 7

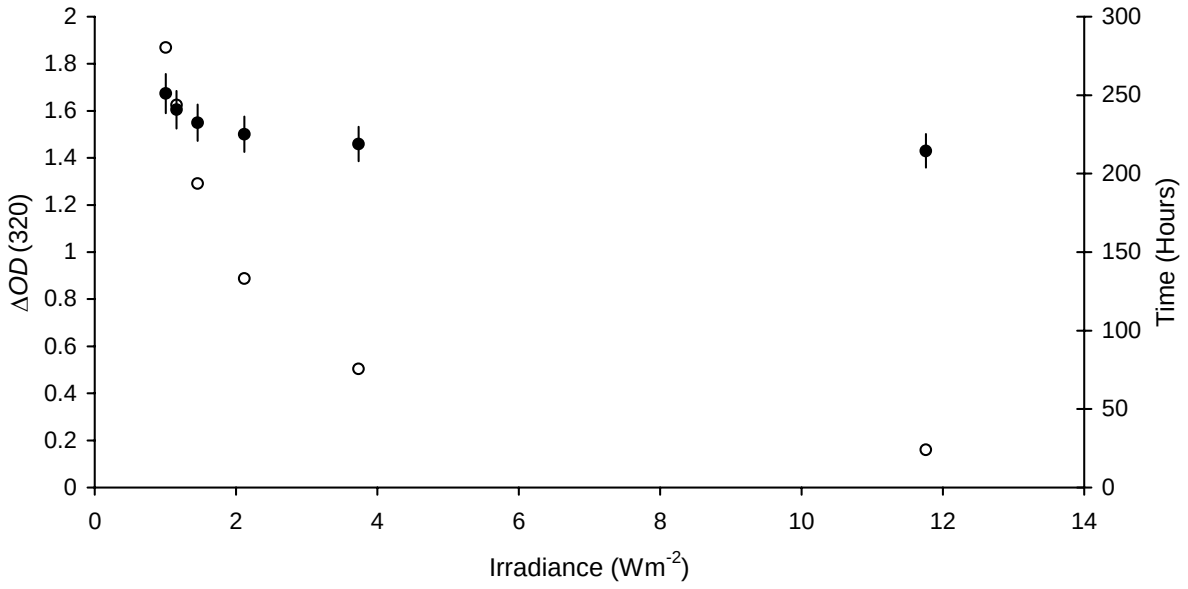
2
1.8
1.6
1.4
1.2
1
0.8
0.6
0.4
0.2
0
ΔOD (320)
300
250
200
150
100
50
0
Time (Hours)
0
2
4
6
8
10
12
14
Irradiance (Wm-2)

Figure 8

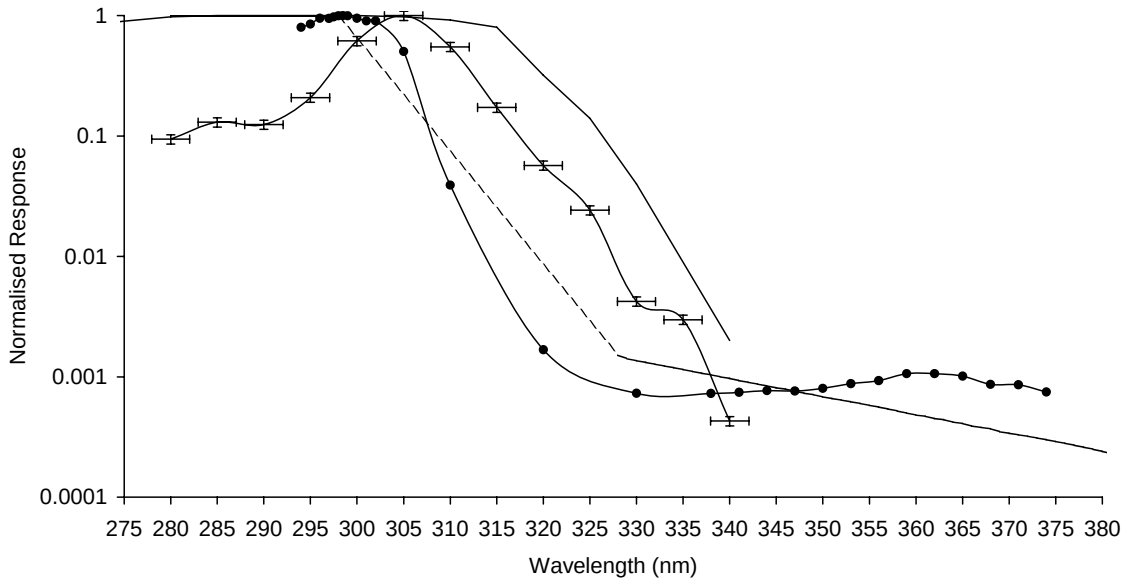
Normalised Response
1
0.1
0.01
0.001
0.0001
275 280 285 290 295 300 305 310 315 320 325 330 335 340 345 350 355 360 365 370 375 380
Wavelength (nm)

Figure 9